Bulletin of the Seismological Society of America, Vol. 101, No. 3, pp. 1371–1385, June 2011, doi: 10.1785/0120100223

Bayesian Estimation of the Spatially Varying Completeness Magnitude of Earthquake Catalogs

by A. Mignan, M. J. Werner,* S. Wiemer, C.-C. Chen, and Y.-M. Wu

Abstract Assessing the completeness magnitude M_c of earthquake catalogs is an essential prerequisite for any seismicity analysis. We employ a simple model to compute M_c in space based on the proximity to seismic stations in a network. We show that a relationship of the form $M_c^{\text{pred}}(d) = ad^b + c$, with d the distance to the kth nearest seismic station, fits the observations well, k depending on the minimum number of stations being required to trigger an event declaration in a catalog. We then propose a new M_c mapping approach, the Bayesian magnitude of completeness (BMC) method, based on a two-step procedure: (1) a spatial resolution optimization to minimize spatial heterogeneities and uncertainties in M_c estimates and (2) a Bayesian approach that merges prior information about M_c based on the proximity to seismic stations with locally observed values weighted by their respective uncertainties. Contrary to the current M_c mapping procedures, the radius that defines which earthquakes to include in the local magnitude distribution is chosen according to an objective criterion, and there are no gaps in the spatial estimation of M_c. The method solely requires the coordinates of seismic stations. Here, we investigate the Taiwan Central Weather Bureau (CWB) seismic network and earthquake catalog over the period 1994–2010.

Introduction

Knowledge of the completeness of earthquake catalogs is crucial for virtually any seismicity analysis (Habermann, 1987). The completeness magnitude, or M_c, is defined as the lowest magnitude at which all earthquakes in a space-time volume are reliably detected (e.g., Rydelek and Sacks, 1989; Woessner and Wiemer, 2005). Studies such as the analysis of rate changes, static and dynamic triggering, mapping of seismicity parameters, earthquake forecasting, and probabilistic seismic hazard assessment commonly require knowledge of the overall M_c of an earthquake catalog.

If the magnitudes of a set of earthquakes obey the Gutenberg–Richter law (Gutenberg and Richter, 1944), M_c can also be defined as the minimum magnitude at which the (complementary) cumulative frequency magnitude distribution (FMD) departs from the exponential decay (e.g., Zuniga and Wyss, 1995). Most existing techniques to estimate M_c follow this second definition, which assumes the validity of the Gutenberg–Richter law, in other words, the self-similarity of earthquakes (e.g., Wiemer and Katsumata, 1999; Wiemer and Wyss, 2000; Cao and Gao, 2002; Marsan, 2003; Kagan, 2002, 2003; Woessner and Wiemer, 2005; Amorèse, 2007; Iwata, 2008). Some notable exceptions are the techniques by Rydelek and Sacks (1989), who estimate M_c by comparing the day-to-night ratio of events per magnitude increment; and those by Schorlemmer and Woessner (2008), who determine earthquake detection probabilities directly from seismic stations recordings and by using noise spectra of seismic stations (e.g., Gomberg, 1991; Kvaerna and Ringdal, 1999; Kvaerna *et al.*, 2002a,b).

Most studies that focus on seismicity features in relatively large regions, for instance, regional earthquake forecasts (e.g., Helmstetter *et al.*, 2007; Wiemer and Schorlemmer, 2007; Werner, Helmstetter, *et al.*, 2011) need to also consider the spatial, and possibly the temporal, variations of M_c. An M_c mapping procedure was proposed by Wyss *et al.* (1999) and discussed in more detail by Wiemer and Wyss (2000). Studies can use such an $M_c(x, y, z, t)$ archive either by directly incorporating the knowledge of M_c at each space-time node in the computation of the seismicity parameter of interest (e.g., Wiemer and Schorlemmer, 2007) or, if one decides to use a single overall M_c cutoff for the whole region of interest, by defining M_c as the highest observed value in space and time. The latter approach considerably decreases the number of available data; however, the $\max(M_c(t, x, y, z))$ approach results in a more accurate value than the bulk value computed from the full data set, especially for areas at the border or outside the seismic network.

As techniques in statistical seismology are becoming more refined, there is an increasing need for robust spatial mapping of M_c. Existing methods, however, are problematic,

*Now at Department of Geosciences, Princeton University.

as pointed out already by Rydelek and Sacks (2003) (but see also Wiemer and Wyss [2003]). The Wiemer and Wyss (2000) approach and its variants (e.g., Woessner and Wiemer, 2005; Hutton *et al.*, 2010) all have two basic limitations:

- L1: an *ad hoc* definition of the spatial resolution of M_c;
- L2: gaps in regions of low seismicity where M_c cannot be computed with confidence.

It is these shortcomings that we address in this study.

An existing solution proposed to overcome these limitations is the Probability-based magnitude of completeness (PMC) method (Schorlemmer and Woessner, 2008; Nanjo, Schorlemmer, *et al.*, 2010; Schorlemmer *et al.*, 2010). PMC uses the phase data, station information, and network-specific attenuation relations to estimate earthquake detection probabilities and does not assume the power-law behavior of seismicity. However, the PMC approach has several drawbacks. First, it is time consuming, requiring a dedicated study and weeks to months of data processing. Second, PMC estimates are not sensitive to temporal changes in M_c, such as during aftershock sequences (J. Woessner, personal comm., 2010). Third, the PMC estimates are sometimes incompatible with Gutenberg–Richter-based estimates (Schorlemmer and Woessner, 2008; Nanjo, Schorlemmer, *et al.*, 2010). Finally, the data necessary for the PMC method are not always available (Hutton *et al.*, 2010).

In the present work, we propose a spatial statistical model of M_c based on the observed relation between M_c and station density, which requires much less information than the PMC method, but which nevertheless solves the aforementioned problems L1 and L2 of M_c maps. Because, *a priori*, the spatial variations of M_c depend to the first order on the local density of seismic stations, we model and estimate the empirical relationship $M_c^{\text{pred}} = f(d)$ between M_c and the distance d to the kth nearest station, where M_c^{pred} is the magnitude of completeness predicted by the model. We first modify the current M_c mapping methodology by estimating the optimal spatial resolution of M_c. We then use a Bayesian method (e.g., Wikle and Berliner, 2007; Werner, Ide, and Sornette, 2011) to combine local M_c observations and their uncertainty with the prior model information, or the predictive relation $M_c^{\text{pred}} = f(d)$.

Earthquake Catalog

We use data from the Central Weather Bureau Seismic Network (CWBSN), which is responsible for monitoring earthquakes in the region of Taiwan. It consists of a central recording system currently with 71 telemetered stations that are equipped with three-component Teledyne/Geotech S13 seismometers. The CWBSN instruments were operating in a triggered-recording mode prior to 1994, when continuous recording began. The network is equipped with a system of automatic earthquake detection followed by manual verification. We refer the reader to Shin and Teng (2001) and Wu, Chang, *et al.* (2008) for more details about the CWBSN.

We selected earthquakes in the CWB earthquake catalog from 1 January 1994 to 31 March 2010 (Fig. 1) with focal depths less than 35 km, which is comparable to the thickness of the seismogenic zone in Taiwan (Wang *et al.*, 1994).

The region of Taiwan is highly appropriate for the purpose of this study for the following reasons: (1) high-quality data with an average M_c of 2.0 (e.g., Wu and Chen, 2007), (2) no major change in the network over a period of 16 yr, (3) evenly distributed seismic stations, and (4) many earthquakes (Taiwan is one of the most seismically active regions in the world, with about 18,000 events recorded each year since 1994 in an approximately 400 km × 550 km region [Wu, Chang, *et al.*, 2008]).

Magnitude uncertainties can lead to deviations from the Gutenberg–Richter law, which may have an impact on M_c estimates. Uncertainties such as systematic errors or random errors can significantly impact the results (Tinti and Mulargia, 1985) because they can lead to magnitude stretches or shifts in the FMD (Habermann, 1987; Zuniga and Wyss, 1995; Zuniga and Wiemer, 1999). Wu *et al.* (2005) showed that the local magnitude M_L used in the CWB did not correlate well with the moment magnitude scale and therefore proposed a corrected relationship, $M_{L_{new}}$. Using this new relationship would lead to a downward shift in all magnitude estimates. However, we used the original magnitudes of the

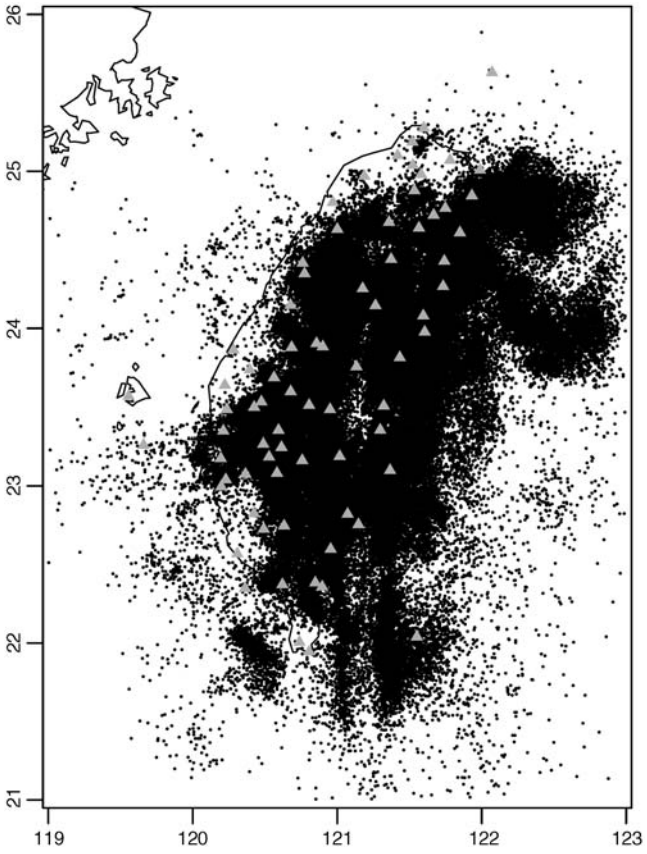

Figure 1. Map of the region of Taiwan with earthquakes listed in the CWB catalog from 1994 to 2010. Seismic stations are represented by triangles.

earthquake catalog because we did not want to add further uncertainties resulting from the conversion to moment magnitudes (see, e.g., Castellaro *et al.*, 2006). Werner and Sornette (2008) discussed and estimated intramagnitude and intermagnitude uncertainties and showed that the distributions of errors have tails that are fatter than Gaussian. While Tinti and Mulargia (1985) observed an upward shift in the Gutenberg–Richter power-law part of the FMD after adding a Gaussian noise to magnitude estimates, we assume in the present work that such errors are systematic and therefore have no role in the spatial variability of M_c. This assumption should, however, be verified in further studies.

Methods for Estimating and Mapping M_c

Nonparametric Techniques to Compute M_c

While a number of techniques exist to compute M_c (see the review by Woessner and Wiemer [2005]), in the present work, we use the nonparametric maximum curvature (MAXC) method (Wyss *et al.*, 1999; Wiemer and Wyss, 2000) because it is robust and simple. However, the Bayesian approach and the *a priori* model we discuss in the following paragraphs can be used with any method.

The MAXC technique is a fast and straightforward way to estimate M_c and consists of finding the magnitude bin with the highest frequency of events in the frequency-magnitude plot. The technique has been shown to underestimate M_c in the case of gradually curved FMDs, which we believe arise from spatiotemporal heterogeneities of the network (Wiemer and Wyss, 2000; Woessner and Wiemer, 2005).

For comparison, we use another nonparametric technique, the median-based analysis of the segment slope (MBASS) method (Amorèse, 2007). The MBASS technique is based on an iterative method that searches for slope changes in the noncumulative FMD; the acceptance or rejection of the null hypothesis (no change in slope) is based on the Wilcoxon rank-sum test. Amorèse (2007) shows that the main discontinuity (where the probability of a change in slope is largest) matches the completeness magnitude M_c estimated by the parametric entire magnitude range (EMR) technique (Woessner and Wiemer, 2005; Hutton *et al.*, 2010; Nanjo, Ishibe, *et al.*, 2010). Because the EMR technique has four free parameters and makes an additional assumption about the incomplete part of the FMD, we do not consider it here.

Figure 2 shows the FMD of the Taiwan CWB catalog as well as the Gutenberg–Richter law fit from magnitudes greater than M_c. We compute M_c by using a Monte Carlo approximation of the bootstrap method (i.e., resampling with replacement; Efron, 1979), as already used in other M_c studies (Woessner and Wiemer, 2005; Amorèse, 2007), and we use $N_s = 200$ bootstrap samples as recommended by Woessner and Wiemer (2005). In this study, we define M_c as the arithmetic mean of M_c values obtained from bootstrapping and σ_0 as its standard error. We compute the b value of the Gutenberg–Richter law by using the maximum-likelihood technique (Aki, 1965) and determine its confidence interval from the M_c standard error σ_0 and the b-value standard error (Shi and Bolt, 1982). If we assume self-similarity, then the MAXC technique underestimates M_c with $M_c^{\text{bulk}}(\text{MAXC}) = 1.98$ ($\sigma_0 = 0.04$) resulting in $b = 0.78$, while the MBASS technique gives an estimate of $M_c^{\text{bulk}}(\text{MBASS}) = 2.37$ ($\sigma_0 = 0.07$), resulting in $b = 0.88$. M_c^{bulk} corresponds to the magnitude of completeness computed from the bulk FMD, in other words, the FMD of the

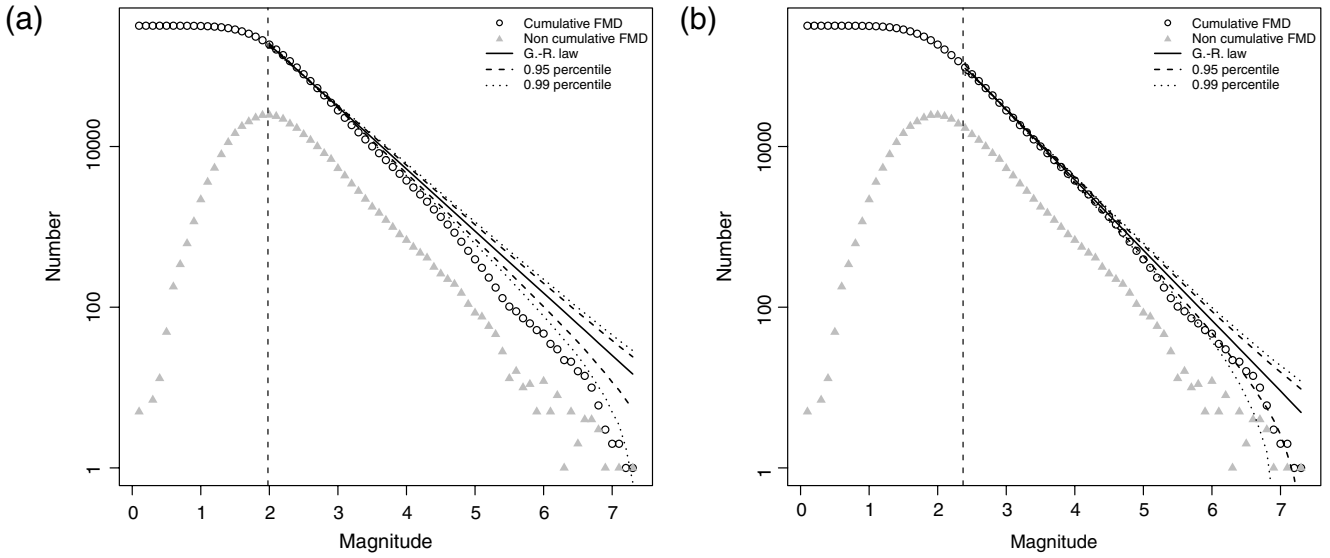

Figure 2. FMD of earthquakes in the Taiwan CWB earthquake catalog during the period 1 January 1994–31 March 2010. The b value, or slope of the Gutenberg–Richter law, is computed for magnitudes greater than M_c (dotted vertical line) by using the maximum-likelihood technique. (a) M_c estimated using the maximum curvature (MAXC) method: $M_c^{\text{bulk}}(\text{MAXC})$ 1.98 with standard error $\sigma_0 = 0.04$, resulting in $b = 0.78$. (b) M_c estimated with the median-based analysis of the segment slope (MBASS): $M_c^{\text{bulk}}(\text{MBASS})$ 2.37 with standard error $\sigma_0 = 0.07$, resulting in $b = 0.88$.

entire earthquake catalog. Visual inspection of Figure 2 confirms that the MAXC bulk estimate is too low; MAXC (by definition) is not sensitive to gradual changes in M_c, as suggested by Woessner and Wiemer (2005).

Characteristics of the Current M_c Mapping Approach

The method to map M_c proposed by Wyss *et al.* (1999) was defined as follows: At each grid node, M_c is calculated from the N closest events to that point, with N fixed. In their study, the authors used the MAXC technique to compute M_c, while Wiemer and Wyss (2000) used the goodness-of-fit test (GFT), a technique that compares the observed FMD with synthetic distributions. Rydelek and Sacks (2003) argued that using a fixed number of events to determine M_c is problematic because the resulting values on the map have an unrealistic and variable relationship to the actual seismicity. This is especially true in areas of high-seismicity density gradients, which is the case in most regional studies with active zones bordered by aseismic ones. Wiemer and Wyss (2000) fixed a maximum radius to limit these discrepancies. Wiemer and Wyss (2003) also explained that the constant number approach has the benefit that the uncertainty in M_c, which scales with the sample size, is less variable across a map. However, they argued that a constant number mapping should be compared to a constant radius mapping to verify that the results are not significantly affected by this choice. Hutton *et al.* (2010) discuss the observed differences between the two approaches in detail for southern California.

The use of a constant radius also introduces problems, which we illustrate by comparing M_c maps computed for Taiwan over the period 1994–2010 for different radii, $r = [5, 10, 20, 50, 75]$ km (Fig. 3). The minimum (or fixed) number of events required at each node depends on the desired robustness of the M_c estimate. Woessner and Wiemer (2005) studied the dependence of M_c on sample size and verified that the uncertainty decreases with an increasing number of events for most techniques (e.g., MAXC, GFT, and EMR techniques).

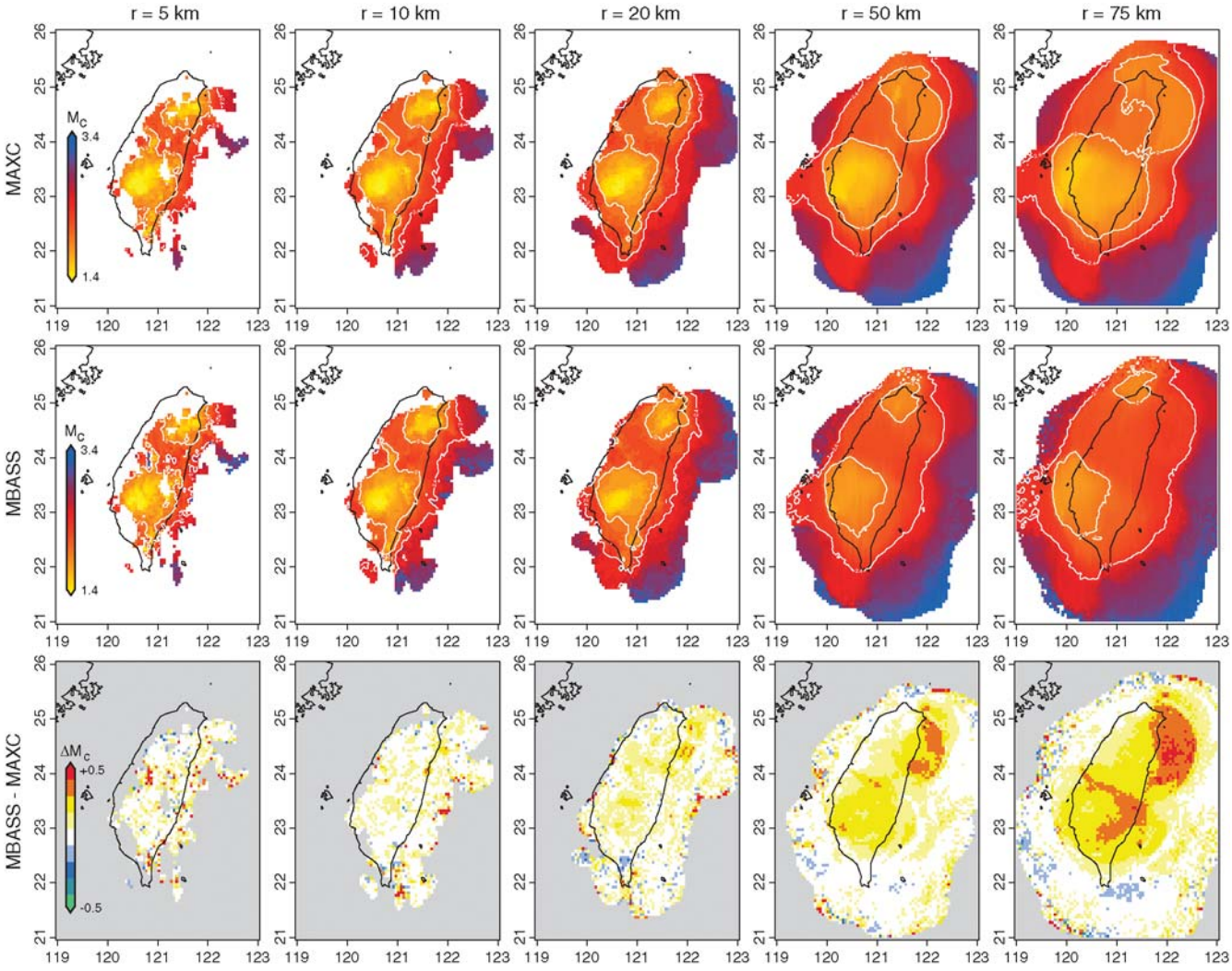

Figure 3. Impact of the radius r on the completeness magnitude M_c in the fixed-radius approach: M_c(MAXC) estimates, M_c(MBASS) estimates, and the difference M_c(MBASS) − M_c(MAXC) are shown in the map view. M_c is computed on a $0.05° \times 0.05°$ grid, using cylinders of radius $r = [5, 10, 20, 50, 75]$ km and a minimum number of $N_{min} = 100$ events. Contours represent M_c 2.0 and M_c 2.4.

Because uncertainty estimates are not used in the current M_c mapping methodology, an educated guess must be made to decide which minimum (or fixed) number of events seems the most reasonable. For the purposes of this section, we fix the minimum number of earthquakes to $N_{min} = 100$. Wyss *et al.* (1999) use the MAXC technique with a fixed number $N_{fix} = 400$ of events. Wiemer and Wyss (2000) use the GFT method with $N_{fix} = 250$ events. Woessner and Wiemer (2005) and Schorlemmer and Woessner (2008) use the EMR technique with $N_{min} = 60$ and 100 events, respectively. Finally, Hutton *et al.* (2010) use the EMR technique with $N_{min} = 100$ events and $N_{fix} = 200$ or 500 events, and Nanjo, Ishibe, *et al.* (2010) with $N_{fix} = 200$ events. To avoid gaps in regions of low seismicity, a lower number of events N_{min} is sometimes tolerated (Woessner and Wiemer, 2005), or a high M_c value is fixed *ad hoc* in regions of little or no data (Wiemer and Schorlemmer, 2007; Hutton *et al.*, 2010).

We observe in Figure 3 that local M_c(MAXC) and M_c(MBASS) values are relatively similar up to $r = 20$ km, but they diverge for larger radii, the discrepancy being maximal for r tending to infinity, in other words, when the completeness magnitude is computed from the FMD of the full earthquake catalog. In that case, the difference in the two M_c estimates is $\Delta M_{cM_c}^{bulk} = 0.4$ (Fig. 2). This suggests that the MAXC technique does not underestimate M_c compared to MBASS results when estimated in regions of homogeneous recording ability of the network. Because the first step of the approach presented in this paper is to minimize the spatial heterogeneities of the network, for the rest of this study, we propose to only use the MAXC technique to estimate M_c.

The fundamental challenge in defining an improved M_c mapping approach that overcomes the shortcomings of the constant N or r approaches is to increase the number of events available to estimate M_c while including only those events from the homogeneous regions of the network in which the same detection threshold is valid. The spatial resolution of M_c estimates should reflect the spatial heterogeneities of the recording network; if neighboring regions are characterized by the same detection capability, then all earthquakes in the joint region should be used to estimate the completeness threshold to reduce uncertainties. This consideration is neglected by the current approach that employs a fixed radius or a fixed number of earthquakes to estimate M_c. When the radius r increases (i.e., when the spatial resolution is reduced), the number of gaps decreases, but differences between MAXC M_c and MBASS M_c estimates increase (Fig. 3). These discrepancies are not incorporated in uncertainty estimates (σ_0), because the latter are reduced when the radius and thus, the sample size, increase.

While the current mapping techniques can lead to reasonable estimates of M_c, users should be aware of the possible bias due to heterogeneities of the network. One possible test is to compare results obtained by MAXC and MBASS for different fixed radii, as shown in Figure 3, and verify that the results do not differ significantly. The educated guess on the fixed radius could hence be improved.

M_c Spatial Resolution Optimization Procedure

High-Resolution M_c Map

To estimate M_c in regions of the same or similar detection probabilities and to thereby reduce possible errors in local M_c and σ_0 estimates, we compute a high-resolution map of M_c values in small, nonoverlapping cells (here on a $0.05° \times 0.05°$ grid) so that the M_c value only depends on the events located within each cell (Fig. 4a), resulting in an M_c map based on disjoint, independent data. (In the Spatial Model of M_c section, we verify that the cell size we chose for Taiwan is smaller than the minimum expected spatial heterogeneity in M_c for the CWBSN). We fix the minimum number of events to $N_{min} = 4$, which is the lowest possible value to get a bounded maximum in the noncumulative FMD curve. Figure 4b shows the corresponding σ_0 map.

Woessner and Wiemer (2005) suggested that a minimum number of $N_{min} = 200$ events were desirable to get reliable estimates of M_c; further statistics should be used to test the significance of the results if fewer events are used in the estimation. Figure 4c shows a scatter plot of the standard error σ_0 versus the number of events n in each independent cell. On average, a larger sample size n decreases the uncertainty of the M_c estimate. One might naively think that the only relevant characteristic of each sample needed to reduce the uncertainty of M_c is the sample size and that, therefore, the small standard errors for small sample size might be unrealistically small. In particular, one might question that an M_c estimate with $\sigma_0(n = 4) = 0.05$ obtained from four events is actually as reliable as an M_c estimate with $\sigma_0(n = 5,000) = 0.05$ obtained from 5000 earthquakes. However, as we show in the Appendix, bootstrapping indeed seems to give reliable uncertainty estimates of M_c for $N_{min} \geq 4$, at least under the assumption of both a particular but reasonable FMD and the MAXC definition of M_c. This can be illustrated by looking at the frequency-magnitude plot of Figure 2a (represented by the gray triangles). For any random sample of size n from the full catalog of size N_{max}, each earthquake has an equal probability of selection n/N_{max}. Thus, the number of occurrences for each magnitude bin is equally reduced at plus or less one event (discrete data), and the magnitude bin with the highest frequency of events (i.e., M_c in the MAXC definition) is likely to remain the same for any n (see simulation results in the Appendix).

Therefore, the large variability of the estimated uncertainty σ_0 for small sample sizes seems real and reflects the extent to which the particular magnitudes of a sample can constrain M_c; in other words, different samples of the same size are not equally informative in constraining M_c when bootstrapped. Therefore, using a generic relationship for the standard error in terms of the sample size, such as $\sigma_0(n) \sim 1/\sqrt{n}$, would lead to an unnecessary loss of information; the standard error determined from bootstrapping reveals more information and is a better estimator of the uncertainty.

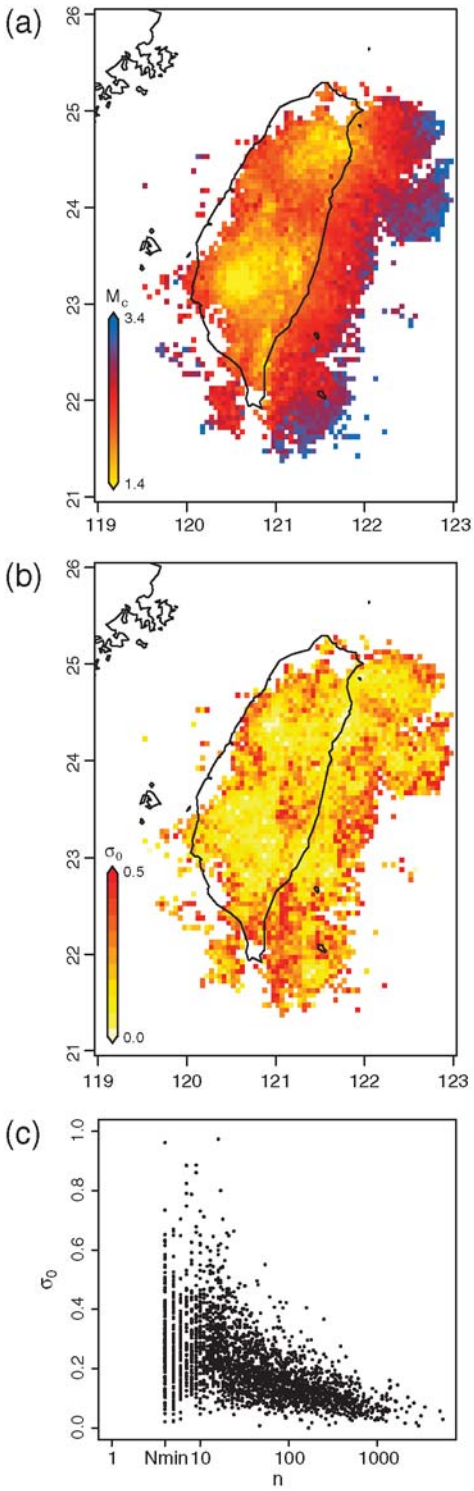

Figure 4. (a) High-resolution M_c map of the Taiwan CWB earthquake catalog for the period 1994–2010. M_c is computed on a $0.05° \times 0.05°$ grid, using all events in the corresponding cells and a minimum number of $N_{min} = 4$ events. (b) Corresponding standard error σ_0 map. (c) σ_0 versus n, the number of events in each cell. σ_0 tends to decrease with increasing n, but the large variability of σ_0 for small samples reflects the fact that different samples provide varying (but accurate) constraints on M_c when bootstrapped (see the Appendix).

Relationship between M_c and Distance to Seismic Stations

We now determine a simple model that predicts an expected M_c based on the density of stations. This model can supplement the estimated M_c values specifically in regions of large uncertainties. Wiemer and Wyss (2000) documented an increase of the completeness magnitude with distance to the fourth nearest station, based on data from California and Alaska. Nanjo, Ishibe, *et al.* (2010) observe a similar feature for Japan. The authors used the distance to the fourth nearest station because it corresponds to the minimum number of stations to be triggered for initiating the location procedure in the Japan Meteorological Agency seismic network. Event location in the Taiwan CWBSN requires at least three stations and at least five phases, *P* or *S*. Therefore, an event is declared only when three or more stations detect it. Note that more stations can be used to decrease location uncertainty and that the *k*th nearest station is not always the *k*th-triggered station (Nanjo, Ishibe, *et al.*, 2010). For Taiwan, it seems equally reasonable to use the distance to the third-, fourth-, or fifth nearest station. All the results and figures presented through this paper are based on a distance to the fifth station. Results for a distance to the third or fourth station are only discussed when necessary. Figure 5a shows that M_c increases with the distance to the fifth station in the CWBSN of Taiwan, in agreement with observations in other regions (Wiemer and Wyss, 2000; Nanjo, Ishibe, *et al.*, 2010).

The dominant frequency of the recorded seismogram, and the frequency of the maximum amplitude peak at which M_L is measured, is dependent on the magnitude. Smaller events will have a higher dominant frequency, and because higher frequencies attenuate faster, the $M_c(d)$ curves shown in Figure 5 are inherently also frequency dependent. Attenuation of seismic waves with distance and scaling with magnitude is, of course, a much-studied subject, as it is used in ground motion prediction equations (GMPEs) and in numerical simulations of wave propagation. However, GMPEs tend to be constrained for larger magnitudes only. Our interest here is to find a simple model based only on the $M_c(d)$ observations because, in this way, we use the observed values as input, averaging over all the complexities of the attenuation (frequency dependence, 3D structure, site amplification, basin effects, etc.).

We determine the relationship $M_c^{pred} = f(d)$ from a nonlinear least-squares regression with d, the distance to the fifth nearest station. For the functional form of f, we choose $ad^b + c$ with $0 < b < 1$, which represents to the first order the just-mentioned geometric dispersion and attenuation of the amplitude of seismic waves with distance from the seismic source. In Figure 5, we show the fit of this functional form to the observations.

Optimized M_c Map

The relationship $M_c^{pred} = f(d)$ shown in Figure 5a indicates that M_c varies more rapidly with distance in the areas of

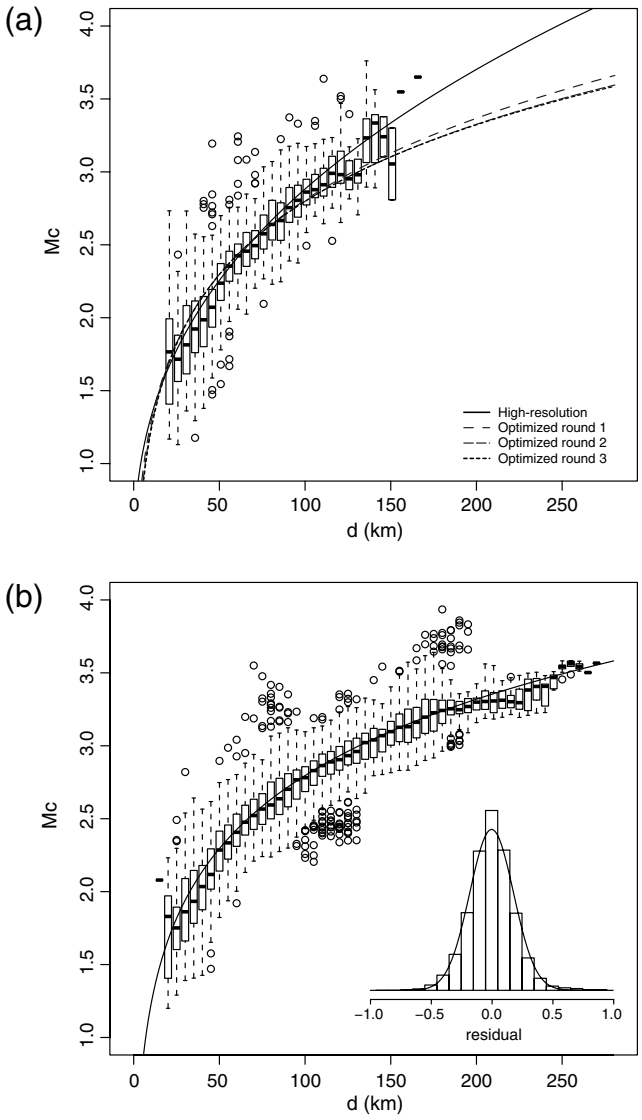

Figure 5. (a) Completeness magnitude M_c as a function of distance d to the fifth nearest seismic station, based on the high-resolution M_c map (Fig. 4a). Boxes represent the range from the first to the third quartiles of all M_c estimates at a given distance. The relationship $M_c^{pred} = f(d)$ is indicated by the solid curve. Modified relationships based on the optimization procedure are shown for comparison. (b) M_c versus d, based on the third round of optimization. The relationship $M_c^{pred} = f(d)$ is indicated by the solid curve (which is equal to the dotted curve in Fig. 5a). The M_c residual distribution $M_c^{pred} - M_c^{obs}$ is fitted by a normal distribution with mean 0.00 and standard deviation $\sigma = 0.18$.

better completeness, the dense inner part of the seismic network, when compared with the sparse outer regions. To quantify this, we can define a variable spatial resolution $\Delta d = g(d)$ of the completeness magnitude:

$$\Delta d = \left(\frac{ad^b + \sigma}{a}\right)^{1/b} - \left(\frac{ad^b - \sigma}{a}\right)^{1/b}, \qquad (1)$$

with a and b defined by $M_c^{pred} = f(d)$ and the standard deviation σ from the residual $M_c^{pred} - M_c^{obs}$. The parameter $\Delta d(d)$ measures a distance over which the completeness magnitude varies by less than two standard deviations and, therefore, cannot be resolved.

Based on this estimate of the spatial resolution of the completeness magnitude, we then locally reestimate M_c by using the events within a cylinder centered on each grid cell with a radius $r = \Delta d/2$. If Δd is smaller than the diagonal of the $0.05° \times 0.05°$ cell, we use all events in that cell. This new variable (but optimized) radius approach is different from the variable radius/constant number approach of Wiemer and Wyss (2000), in which the size of the cylinder depends on the density of earthquakes. In our approach, the size of the cylinder is an estimate of the possible resolution of the completeness magnitude in space.

From the refined M_c estimates at each grid node, we then reestimate the parameters of the function f and reiterate i times until the difference $f_{i+1}(d) - f_i(d)$ becomes insignificant. The spatial model estimated from the high-resolution M_c map is only constrained for $d < 160$ km (Fig. 5a). Once a new M_c map is computed, the model can be reestimated from a larger range of d. We stop after the third iteration (Fig. 5b), when the root mean square error of $f_{i+1}(d) - f_i(d)$ is less than 0.2 for all d, and obtain an optimized M_c map. $f_{i+1}(d)$ becomes indistinguishable from $f_i(d)$ after the third iteration. The smallest distance we find is $d_{min} = 15$ km, which corresponds to the smallest distance of any earthquake to its fifth nearest station in the Taiwan CWBSN. To constrain the model over smaller values of d, we would need a denser seismic network.

Figure 6a,b shows the optimized M_c and σ_0 maps, respectively. Compared to the high-resolution maps of Figure 4, the area over which we could obtain M_c estimates is greatly expanded, and the uncertainties σ_0 are reduced because the number of events used to compute the local M_c is maximized while possible errors due to spatial heterogeneities are minimized.

Bayesian Approach

Spatial Model of M_c

We can use the empirical relationship $M_c^{pred} = f(d)$ as a simple predictive spatial model of the completeness magnitude. After the third iteration of the optimization, we find

$$M_c^{pred}(d) = 9.42d^{0.0598} - 9.60, \qquad \sigma = 0.18, \qquad (2)$$

where d is the distance to the fifth nearest station. The residual of the spatial model $M_c^{pred} - M_c^{obs}$ can be fitted by a normal distribution with mean 0.00 and standard deviation $\sigma = 0.18$ (Fig. 5b). Note that we find $M_c^{pred}(d, k = 4) = 5.96d^{0.0803} - 5.80$, $\sigma = 0.18$ and $M_c^{pred}(d, k = 3) = 4.81d^{0.0883} - 4.36$, $\sigma = 0.19$ for d, the distance to the kth nearest station. By using the parameters of equation (2) in equation (1), we can verify that M_c spatial variations may be resolved down to $\Delta d \approx 8$ km for Taiwan (computed using $d_{min} = 15$ km), which is larger than the grid resolution

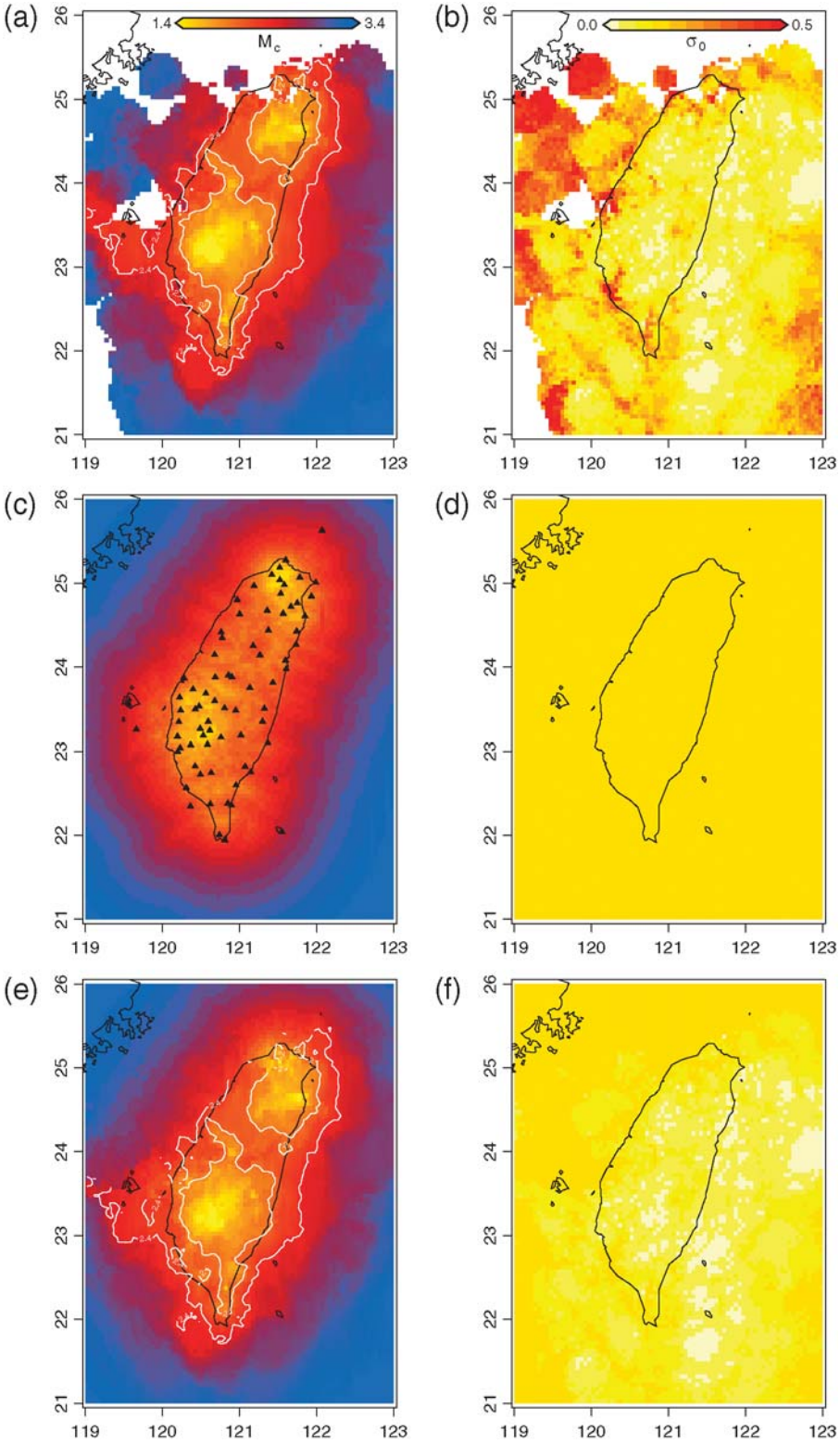

Figure 6. Bayesian estimation of the completeness magnitude of the Taiwan CWB catalog for the period 1994–2010. (a) Observed M_c^{obs} map obtained from locally optimized radii. (b) Respective uncertainty map σ_0. (c) M_c^{pred} map predicted from prior knowledge of the completeness magnitude based on the proximity to seismic stations (represented by triangles). (d) Respective standard deviation map σ. (e) BMC map, or posterior completeness magnitude M_c^{post}, after optimally merging observed and predicted values, weighted by their uncertainties. (f) Respective standard deviation map σ^{post}. Contours represent M_c 2.0 and M_c 2.4.

of $0.05° \times 0.05°$ (~5 km). In the outer regions of the network, $\Delta d \approx 100$ km. Figure 6c,d shows the predicted M_c and σ maps derived from equation (2) using the spatial distribution of stations in the Taiwan CWBSN.

Bayes' Theorem

In a Bayesian approach, the observed empirical relationship between the completeness magnitude and the proximity to the seismic stations can be used as *a priori* information, or as a forecast model, described by the prior probability distribution $p(M_c)$. Local completeness estimates based on observed magnitudes can be expressed by the conditional data likelihood $p(M_c^{obs}|M_c)$, which accounts for observational uncertainties in the local completeness estimate. The best estimate of the completeness, which employs both the prior information and the local observation, each weighted by their uncertainty, is given by the posterior distribution in Bayes' theorem

$$p(M_c|M_c^{obs}) = \frac{p(M_c^{obs}|M_c)p(M_c)}{p(M_c^{obs})}, \tag{3}$$

where $p(M_c^{obs})$ is the marginal distribution, which can be thought of as a normalizing constant (e.g., Wikle and Berliner, 2007; Werner, Ide, and Sornette, 2011).

How should we parameterize these distributions? As we showed in the previous paragraphs (and in Figure 5b), the residual between the predicted and the observed completeness magnitude $M_c^{pred} - M_c^{obs}$ is well approximated by a Gaussian distribution. We therefore define the prior probability distribution as

$$p(M_c) = \frac{1}{\sqrt{2\pi}\sigma} \exp \frac{-(M_c - M_c^{pred})^2}{2\sigma^2}, \tag{4}$$

where $M_c^{pred} = ad^b + c$ with $a = 9.42$, $b = 0.0598$, $c = -9.60$ (equation 2), and $\sigma = 0.18$ (Fig. 5b). We also assume the conditional data likelihood to be Gaussian (see the Appendix for the validation of this assumption):

$$p(M_c^{obs}|M_c) = \frac{1}{\sqrt{2\pi}\sigma_0} \exp \frac{-(M_c^{obs} - M_c)^2}{2\sigma_0^2}, \tag{5}$$

where M_c^{obs} is the locally observed value based on the optimal local radius (obtained from the spatial resolution optimization procedure) and σ_0 is the local standard error computed from bootstrapping.

With the prior and data likelihood defined as in equations (4) and (5), the posterior in equation (3) simply becomes the product of two Gaussian distributions, and we can thus write the average completeness magnitude M_c^{post} of the posterior as

$$M_c^{post} = \frac{M_c^{pred}\sigma_0^2 + M_c^{obs}\sigma^2}{\sigma^2 + \sigma_0^2}, \tag{6}$$

which is the average of the predicted and observed completeness magnitude, weighted according to their respective uncertainties. The posterior standard deviation σ^{post} is given by

$$\sigma_{post} = \sqrt{\frac{\sigma^2\sigma_0^2}{\sigma^2 + \sigma_0^2}}. \tag{7}$$

Figure 6e,f shows the posterior M_c and σ_0 maps, respectively. Note that we henceforth refer to the posterior M_c maps as Bayesian magnitude of completeness (BMC) maps. From equation (6), we see that M_c^{post} equals M_c^{pred} in cells without data, where the uncertainty of the observed value would be infinite. For other cells, the higher the uncertainty of M_c^{obs} estimates, the higher the weight of M_c^{pred}. Uncertainties are again substantially decreased because of the fusion of M_c estimates with the prior information. It is worth noting that the main features observed in the BMC map shown in Figure 6e are similar to the ones observed with the standard mapping approach (except for the gaps) when a reasonable fixed radius is chosen (Fig. 3). These main features are illustrated here by the $M_c = 2.0$ and $M_c = 2.4$ contours. Moreover, we verified that BMC maps obtained using the distance to the third of fourth nearest station are almost undistinguishable to the map obtained with a distance to the fifth nearest station.

Discussion

Statistical seismology as well as probabilistic seismic hazard assessment relies on robust and readily available models of the completeness of reporting of earthquake catalogs. We introduce a novel approach, the BMC method, to map M_c in space. BMC overcomes some of the limitations of previous mapping approaches. The most substantial innovation of BMC is that we exploit Bayes' theorem to combine in an optimal way the observed M_c at each node with a generic M_c model (Fig. 6). Combining the observed M_c with a model helps specifically in regions of low seismicity rate and low station density, where M_c can only be determined with a high uncertainty. Different from previous Gutenberg–Richter–based approaches (e.g., Woessner and Wiemer, 2005), the final BMC maps thus cover the entire study region, and the uncertainty at each node is minimized. The BMC maps are thus more versatile and robust than previously available Gutenberg–Richter–based approaches. At the same time, the approach is relatively lightweight: A rough BMC study can be performed for any given region within a few hours and only requires an available catalog and the spatial distribution of stations. The PMC method, on the other hand (Schorlemmer and Woessner, 2008; Nanjo, Schorlemmer, *et al.*, 2010), requires much more time for data acquisition, with an access to all picks at all stations.

Both BMC and PMC will produce a model of the spatial distribution of M_c. The BMC model is, by design, much more simplistic, as it does not differentiate between the capability of detection for each station in the way PMC does.

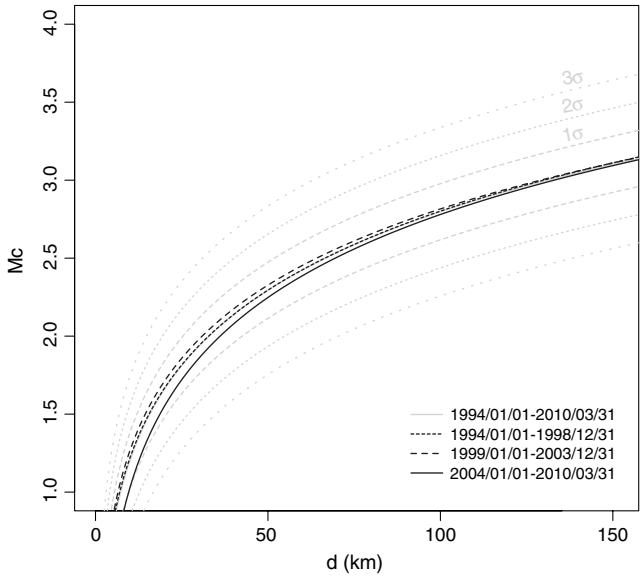

Figure 7. Consistency of the model $M_c = f(d)$ for different time windows. The model (see equation 2) is represented in gray and corresponds to the fit obtained for the period 1994–2010 (see Fig. 5b). Deviations from the model are insignificant for the periods 1994–1998 and 1999–2003. For the period 2004–2010, M_c tends to decrease faster with decreasing d, but remains within the 1σ confidence range.

Nevertheless, the BMC model can be used in the same way as PMC to investigate and plan enhancements to existing seismic networks by placing virtual stations and investigating their impact on the completeness (Nanjo, Schorlemmer, *et al.*, 2010). BMC and PMC make substantially different assumptions: BMC is based on the FMD and assumes a Gutenberg–Richter behavior, while PMC does not. Therefore, if one is interested in specifically looking for deviations from the Gutenberg–Richter law, PMC may be the adequate choice. On the other hand, if one seeks to map b values, the BMC method offers the benefit of inherent compatibility with the computation of b.

Another benefit of the BMC approach lies in eliminating the fixed-radius or fixed-number mapping approach, which was used in all previous applications (Fig. 3). Our iterative procedure strives to find an optimized spatial resolution based on the density of seismic stations. This approach will make the sampling volumes as large as feasible given the local gradient in M_c (Fig. 5).

The functional form we choose to represent the dependence of M_c on station density (equation 2; Fig. 5) is simple by design and only very generally captures the physical processes governing attenuation with distance. Because a more physics-based attenuation model would need to consider frequency dependence, scaling with magnitude, 3D effects, and more, we consider the simple functional form that fits the $M_c(d)$ data directly as a simpler but more constrained approach. One of the potential shortcomings of this approach is that our model may not be very accurate when it is extrapolated beyond the data range on which it is based.

Seismic Network Coverage in Taiwan

High-resolution spatial variations of magnitude completeness in the CWBSN of Taiwan have not been discussed in the literature so far. We present a number of M_c maps for the region of Taiwan over the period 1994–2010, first, using the common mapping method developed by Wiemer and Wyss (2000) for different spatial resolutions and for two techniques, MAXC and MBASS (Fig. 3), and second, using the newly proposed BMC method (Fig. 6).

A comparison of the M_c maps obtained by the two different mapping approaches shows that one could use the constant radius approach with $R_{fix} = 20$ km to get a reasonable

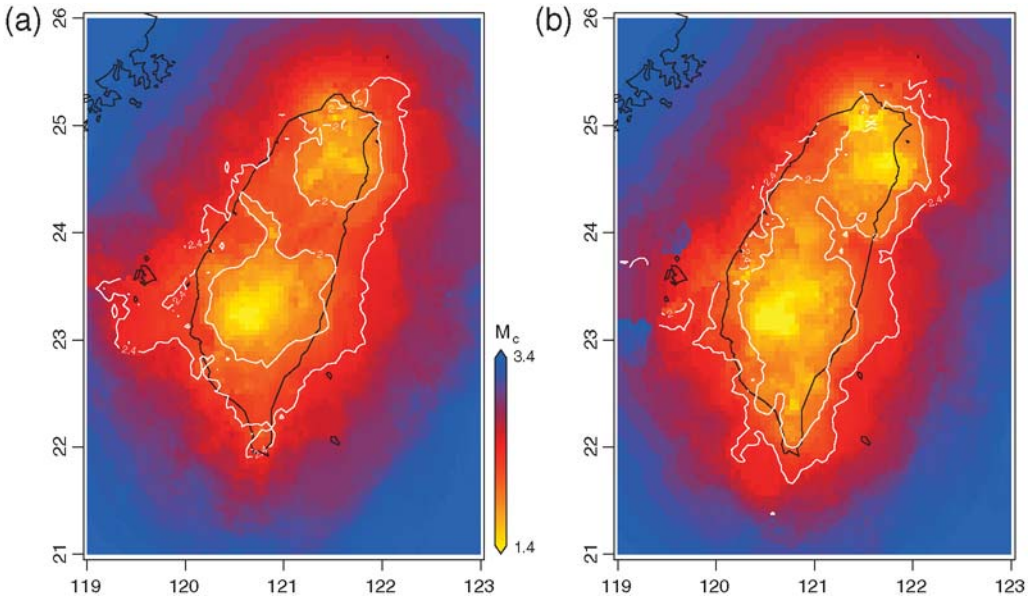

Figure 8. BMC maps (i.e., maps of the posterior completeness magnitude M_c^{post}) for the period (a) 1994–2003 and (b) 2004–2010.

idea of the magnitude of completeness in Taiwan (see M_c contours in Figs. 3 and 6e), irrespective of whether one is using MBASS or MAXC. However, the BMC map (Fig. 6e) shows a higher resolution of M_c in the dense part of the network, which allows for finer seismicity analyses of inland Taiwan. In contrast, past studies investigating seismicity patterns in Taiwan usually considered only one magnitude cutoff for the region of interest (Chen *et al.*, 2005, 2006; Chen and Wu, 2006; Wu and Chiao, 2006; Wu and Chen, 2007; Wu, Chen, and Rundle, 2008). The BMC map shows that the completeness magnitude for inland Taiwan is $M_c \approx 2.4$ over the period 1994–2010, as highlighted by the white outer contour of Figure 6e. Note that M_c can be as low as 1.4 locally (areas shown in yellow).

Nanjo, Ishibe, *et al.* (2010) describe the improvement of the seismic network of the Japanese Meteorological Agency by computing M_c maps for different periods of time. In the case of Taiwan, the network remains almost unchanged over the past 16 yr. We tested the BMC method for different time windows. We verified that deviations from the model of equation (2) were insignificant (i.e., lower than the magnitude increment of 0.1) for any distance d for most periods tested, except for time windows starting in 2004. For the period 2004–2010, M_c decreases by more than 0.1 units in the low d range, although the estimate remains within the 1σ limit (Fig. 7). This general agreement suggests that the model (equation 2) is robust.

According to the staff of the CWB, the network in itself did not change over the period 1994–2010, but a change in the recording system was made after 2003: The continuous recording sampling rate increased from 50 to 100 samples per second. This could explain the deviation observed in the model for the corresponding period. Figure 8 shows BMC maps for the periods 1994–2003 and 2004–2010. While the conservative estimate $M_c = 2.4$ remains valid for inland Taiwan for any period of time, starting in 2004, M_c has been improved in most parts of the country, in agreement with the deviation observed in Figure 7. Therefore, we recommend that users perform seismicity analyses over the period 2004–2010 to maximize the number of low-magnitude events (Fig. 8b). If a longer time frame is required for the seismicity analysis, the user should combine the two BMC maps from Figure 8 and keep the maximum M_c value for each cell to get a conservative estimate, as already proposed by Nanjo, Schorlemmer, *et al.* (2010) when using the PMC method.

Applicability to Other Regions

The BMC method can be applied in any region where coordinates of seismic stations of the relevant network are available. However, depending on the spatial distribution of the stations and earthquake density, the relationship $M_c^{\text{pred}} = f(d)$ may or may not be well constrained. Optimal conditions for constraining the model include (1) many earthquakes, (2) an even coverage of seismic stations in space, and (3) no significant spatiotemporal changes in the seismic network, such as the addition of temporary local networks.

If the parameters of the model cannot be well constrained from a particular regional data set, we propose to directly use equation (2) with the parameter values estimated here as a first-order estimate and to follow the same two-step procedure. This assumes that differences in seismic signal attenuation between Taiwan and other regions do not significantly corrupt the relationship $M_c^{\text{pred}} = f(d)$. This should be verified by comparing different regional spatial models of M_c.

Deviations from the Proposed M_c Model

For the sake of simplicity and conciseness, the proposed model does not take into account changes of the completeness

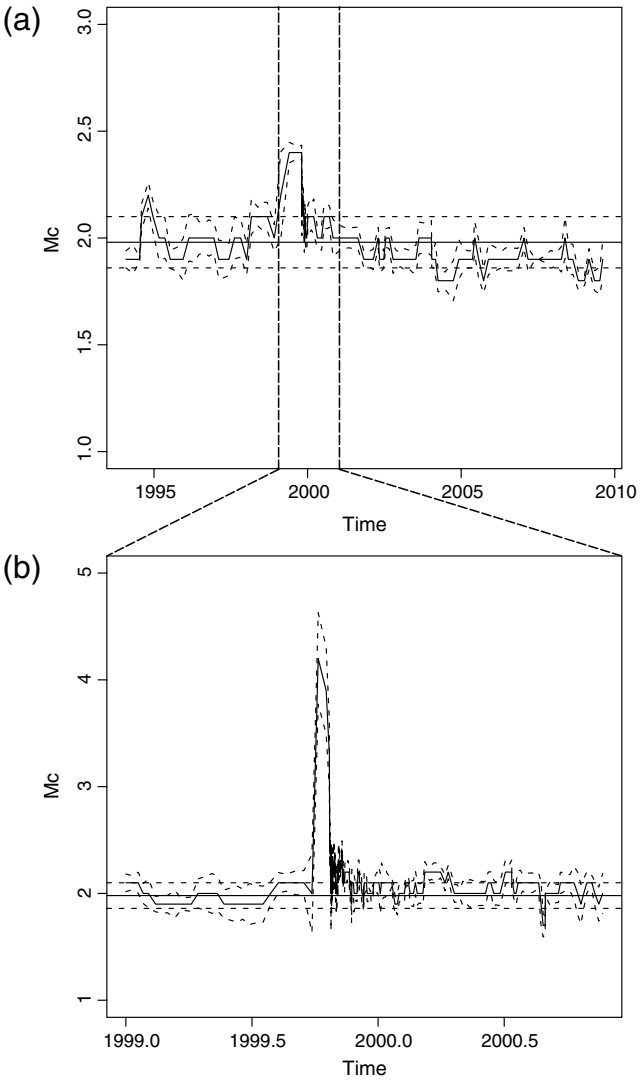

Figure 9. M_c versus time using the Taiwan CWB catalog. Moving window approach (a) with window of size $S = 10,000$ events, moving every 2500 events and (b) $S = 1,000$ events, moving every 250 events. The solid curve represents the mean M_c value, and the dashed curves the 99% confidence bounds. Horizontal lines correspond to M_c^{bulk}(MAXC) and associated 99% confidence bounds (see Fig. 2a).

magnitude of the Taiwan CWB seismic network with depth. Our mapping approach consists of computing M_c from all events located in vertical cylinders centered on each grid cell, as done in earlier studies (e.g., Wiemer and Wyss, 2000; Schorlemmer and Woessner, 2008; Hutton *et al.*, 2010). If we use a maximum depth of 5 km, similar to the cell width of 0.05°, instead of 35 km, M_c tends to be slightly lower in the dense part of the network. In the present work, we prefer to use epicentral locations, which leads to a conservative estimate of M_c. The influence of hypocentral locations on the spatial M_c model should be investigated in the future and compared to results from studies mapping M_c cross sections (e.g., Wiemer and Wyss, 2000). A relocated catalog should also be used to minimize the impact of the error on hypocentral locations (Wu, Chang, *et al.*, 2008).

Figure 9 shows a plot of M_c versus time for the Taiwan CWB earthquake catalog. We used a moving window approach to compute M_c, as done by Woessner and Wiemer (2005). We see that M_c remains stationary for most of the period 1994–2010, in agreement with the fact that the CWBSN remained stable during that time. We note a temporary increase in M_c of several magnitudes because some events are too small to be detected in the coda of the 1999 M_w 7.6 Chi-Chi earthquake and its aftershock sequence (Shin and Teng, 2001). Such a temporary change in M_c is not accounted for in our model, which assumes that all seismic stations have approximately constant detection ability over time. Nonetheless, we see that the M_c changes in 1999 do not perturb the value of M_c^{bulk} (computed for the full time period; see Fig. 2a), in agreement with the observation that MAXC underestimates the completeness magnitude when spatiotemporal heterogeneities are present. In the present case, it allows us to filter the effects of the Chi-Chi earthquake.

To model the effect of episodic large earthquakes on M_c, another approach should be used (e.g., Iwata, 2008), or our model should be improved to take into account variable detection abilities at each seismic station. Regarding this source of error, we also observe that the completeness magnitude was slightly higher during daytime because human activity increases the noise-to-signal ratio (Rydelek and Sacks, 1989). Finally, contrary to the PMC approach (Schorlemmer and Woessner, 2008), we did not take into account the on/off time of stations, which could change our M_c results locally. We suspect that in the case of the Taiwan earthquake, the influence will be small because of the stability of the network over the period 1994–2010.

Conclusions

We proposed a simple model to compute the completeness magnitude M_c in space, based on the distribution of seismic stations. We obtain the following relationship from the 1994–2010 Taiwan CWB earthquake catalog:

$$M_c^{\text{pred}}(d, k = 5) = 9.42d^{0.0598} - 9.60, \qquad \sigma = 0.18,$$

$$M_c^{\text{pred}}(d, k = 4) = 5.96d^{0.0803} - 5.80, \qquad \sigma = 0.18,$$

$$M_c^{\text{pred}}(d, k = 3) = 4.81d^{0.0883} - 4.36, \qquad \sigma = 0.19,$$

where d is the distance to the kth nearest seismic station, and σ is the standard deviation of the M_c estimate.

We then described a new M_c mapping approach, the BMC method, which consists of two steps, (1) a spatial resolution optimization procedure to minimize spatial heterogeneities and uncertainties in M_c estimates, and (2) a Bayesian approach to take into account prior information based on the seismic network configuration as well as the observed local M_c values and their respective uncertainties.

BMC shows a number of improvements compared to the M_c mapping approach proposed by Wyss *et al.* (1999) and used in many other studies (e.g., Wiemer and Wyss, 2000; Woessner and Wiemer, 2005; Hutton *et al.* 2010):

- No gaps in the spatial estimation of M_c and its uncertainty,
- Higher resolution of M_c in the dense part of the seismic network,
- Minimal errors in M_c and σ_0 estimates due to spatial heterogeneities,
- No assumption or educated guess required to set the input parameters r and $N_{\min}$.

Studies investigating seismicity patterns in Taiwan, such as possible precursors to large earthquakes, usually consider only one magnitude cutoff for the whole region (Chen *et al.*, 2005, 2006; Chen and Wu, 2006; Wu and Chiao, 2006; Wu and Chen, 2007; Wu, Chen, and Rundle, 2008). We recommend using a variable $M_c(x, y)$, as shown in the BMC maps of Figure 8.

Our approach can be applied in any region for which the coordinates of seismic stations are available. If no spatial model can be derived for a given region due to poor data, we propose to directly use the relationship $M_c^{\text{pred}} = f(d)$ found for Taiwan as a first-order estimate.

Data and Resources

The earthquake catalog used in this study was provided by the Central Weather Bureau, the government meteorological research and forecasting institution of Taiwan (R.O.C.).

Acknowledgments

The authors wish to thank Associate Editor Martin C. Chapman, as well as Yan Kagan and an anonymous reviewer who supplied numerous constructive comments, resulting in a much-improved paper. The authors are also grateful to Jochen Woessner for reading the manuscript before submittal. This project was partially funded by the Sino-Swiss Science and Technology Cooperation. M. J. Werner was supported by the Competence Center Environment and Sustainability (CCES) project EXTREMES of ETH.

References

Aki, K. (1965). Maximum likelihood estimate of b in the formula $\log N = a - bM$ and its confidence limits, *Bull. Earthq. Res. Inst. Tokyo Univ.* **43,** 237–239.

Amorèse, D. (2007). Applying a change-point detection method on frequency-magnitude distributions, *Bull. Seismol. Soc. Am.* **97,** doi 10.1785/0120060181.

Cao, A. M., and S. S. Gao (2002). Temporal variations of seismic b-values beneath northeastern Japan island arc, *Geophys. Res. Lett.* **29,** doi 10.1029/2001GL013775.

Castellaro, S., F. Mulargia, and Y. Y. Kagan (2006). Regression problems for magnitudes, *Geophys. J. Int.* **165,** doi 10.1111/j.1365-246X.2006.02955.x.

Chen, C.-C., and Y.-X. Wu (2006). An improved region-time-length algorithm applied to the 1999 Chi-Chi, Taiwan earthquake, *Geophys. J. Int.* **166,** doi 10.1111/j.1365-246X.2006.02975.x.

Chen, C.-C., J. B. Rundle, J. R. Holliday, K. Z. Nanjo, D. L. Turcotte, S.-C. Li, and K. F. Tiampo (2005). The 1999 Chi-Chi, Taiwan, earthquake as a typical example of seismic activation and quiescence, *Geophys. Res. Lett.* **32,** L22315, doi 10.1029/2005GL023991.

Chen, C.-C., J. B. Rundle, H.-C. Li, J. R. Holliday, D. L. Turcotte, and K. F. Tiampo (2006). Critical point theory of earthquakes: Observation of correlated and cooperative behavior on earthquake fault systems, *Geophys. Res. Lett.* **33,** L18302, doi 10.1029/2006GL027323.

Efron, B. (1979). 1977 Rietz lecture, bootstrap methods—Another look at the jackknife, *Ann. Stat.* **7,** 1–26.

Gomberg, J. (1991). Seismicity and detection/location threshold in the Southern Great Basin seismic network, *J. Geophys. Res.* **96,** 16,401–16,414.

Gutenberg, B., and C. F. Richter (1944). Frequency of earthquakes in California, *Bull. Seismol. Soc. Am.* **34,** 184–188.

Habermann, R. E. (1987). Man-made changes of seismicity rates, *Bull. Seismol. Soc. Am.* **77,** 141–159.

Helmstetter, A., Y. Y. Kagan, and D. D. Jackson (2007). High-resolution time-independent grid-based forecast for $M \geq 5$ earthquakes in California, *Seismol. Res. Lett.* **78,** 78–86.

Hutton, K., J. Woessner, and E. Hauksson (2010). Earthquake monitoring in Southern California for seventy-seven years (1932–2008), *Bull. Seismol. Soc. Am.* **100,** doi 10.1785/0120090130.

Iwata, T. (2008). Low detection capability of global earthquakes after the occurrence of large earthquakes: Investigation of the Harvard CMT catalogue, *Geophys. J. Int.* **174,** doi 10.1111/j.1365-246X.2008.03864.x.

Kagan, Y. Y. (2002). Seismic moment distribution revisited: I. Statistical results, *Geophys. J. Int.* **148,** 520–541.

Kagan, Y. Y. (2003). Accuracy of modern global earthquake catalogs, *Phys. Earth Planet. In.* **135,** 173–209, doi 10.1016/S0031-9201(02)00214-5.

Kvaerna, T., and F. Ringdal (1999). Seismic threshold monitoring for continuous assessment of global detection capability, *Bull. Seismol. Soc. Am.* **89,** 4, 946–959.

Kvaerna, T., F. Ringdal, J. Schweitzer, and L. Taylor (2002a). Optimized seismic threshold monitoring—Part 1: Regional processing, *Pure Appl. Geophys.* **159,** 969–987.

Kvaerna, T., F. Ringdal, J. Schweitzer, and L. Taylor (2002b). Optimized seismic threshold monitoring—Part 2: Teleseismic processing, *Pure Appl. Geophys.* **159,** 989–1004.

Marsan, D. (2003). Triggering of seismicity at short timescales following Californian earthquakes, *J. Geophys. Res.* **108,** doi 10.1029/2002JB001946.

Nanjo, K. Z., T. Ishibe, H. Tsuruoka, D. Schorlemmer, Y. Ishigaki, and N. Hirata (2010). Analysis of the completeness magnitude and seismic network coverage of Japan, *Bull. Seismol. Soc. Am.* **100,** doi 10.1785/0120100077.

Nanjo, K. Z., D. Schorlemmer, J. Woessner, S. Wiemer, and D. Giardini (2010). Earthquake detection capability of the Swiss Seismic network, *Geophys. J. Int.* **181,** doi 10.1111/j.1365-246X.2010.04593.x.

Ogata, Y., and K. Katsura (1993). Analysis of temporal and spatial heterogeneity of magnitude frequency distribution inferred from earthquake catalogues, *Geophys. J. Int.* **113,** 727–738.

Rydelek, P. A., and I. S. Sacks (1989). Testing the completeness of earthquake catalogs and the hypothesis of self-similarity, *Nature* **337,** 251–253.

Rydelek, P. A., and I. S. Sacks (2003). Comment on "Minimum magnitude of completeness in earthquake catalogs: Examples from Alaska, the Western United States, and Japan," by Stefan Wiemer and Max Wyss, *Bull. Seismol. Soc. Am.* **93,** 1862–1867.

Schorlemmer, D., and J. Woessner (2008). Probability of detecting an earthquake, *Bull. Seismol. Soc. Am.* **98,** doi 10.1785/0120070105.

Schorlemmer, D., F. Mele, and W. Marzocchi (2010). A completeness analysis of the National Seismic network of Italy, *J. Geophys. Res.* **115,** doi 10.1029/2008JB006097.

Shi, Y., and B. A. Bolt (1982). The standard error of the magnitude-frequency b-value, *Bull. Seismol. Soc. Am.* **72,** 1677–1687.

Shin, T.-C., and T.-L. Teng (2001). An overview of the 1999 Chi-Chi, Taiwan, earthquake, *Bull. Seismol. Soc. Am.* **91,** 895–913.

Tinti, S., and F. Mulargia (1985). Effects of magnitude uncertainties on estimating the parameters in the Gutenberg-Richter frequency-magnitude law, *Bull. Seismol. Soc. Am.* **75,** 1681–1697.

Wang, J. H., K. C. Chen, and T. Q. Lee (1994). Depth distribution of shallow earthquakes in Taiwan, *J. Geol. Soc. China* **37,** 125–142.

Werner, M. J., and D. Sornette (2008). Magnitude uncertainties impact seismic rate estimates, forecasts, and predictability experiments, *J. Geophys. Res.* **113,** B08302, doi 10.1029/2007JB005427.

Werner, M. J., K. Ide, and D. Sornette (2011). Earthquake forecasting based on data assimilation: Sequential Monte Carlo methods for renewal processes, *Nonlinear Process. Geophys.* **18,** 49–70, doi 10.5194/npg-18-49-2011.

Werner, M. J., A. Helmstetter, D. D. Jackson, and Y. Y. Kagan (2011). High-resolution long-term and short-term earthquake forecasts for California, *Bull. Seismol. Soc. Am.* **101,** 4, in press.

Wiemer, S., and K. Katsumata (1999). Spatial variability of seismicity parameters in aftershock zones, *J. Geophys. Res.* **104,** 13,135–13,151.

Wiemer, S., and D. Schorlemmer (2007). ALM: An asperity-based likelihood model for California, *Seismol. Res. Lett.* **78,** 134–140.

Wiemer, S., and M. Wyss (2000). Minimum magnitude of complete reporting in earthquake catalogs: Examples from Alaska, the Western United States, and Japan, *Bull. Seismol. Soc. Am.* **90,** 859–869.

Wiemer, S., and M. Wyss (2003). Reply to "Comment on 'Minimum magnitude of completeness in earthquake catalogs: Examples from Alaska, the Western United States, and Japan' by Stefan Wiemer and Max Wyss," by Paul A. Rydelek and Sacks I. S., *Bull. Seismol. Soc. Am.* **93,** 1868–1871.

Wikle, C. K., and L. M. Berliner (2007). A Bayesian tutorial for data assimiliation, *Phys. D Nonlinear Phenom.* **230,** doi 10.1016/j.physd.2006.09.017.

Woessner, J., and S. Wiemer (2005). Assessing the quality of earthquake catalogues: Estimating the magnitude of completeness and its uncertainty, *Bull. Seismol. Soc. Am.* **95,** doi 10.1785/0120040007.

Wu, Y.-M., and C.-C. Chen (2007). Seismic reversal pattern for the 1999 Chi-Chi, Taiwan, M_w 7.6 earthquake, *Tectonophys.* **429,** doi 10.1016/j.tecto.2006.09.015.

Wu, Y.-M., and L. Y. Chiao (2006). Seismic Quiescence before the 1999 Chi-Chi, Taiwan M_w 7.6 Earthquake, *Bull. Seismol. Soc. Am.* **96,** doi 10.1785/0120050069.

Wu, Y.-M., R. M. Allen, and C.-F. Wu (2005). Revised M_L determination for crustal earthquakes in Taiwan, *Bull. Seismol. Soc. Am.* **95,** doi 10.1785/0120050043.

Wu, Y.-M., C.-H. Chang, L. Zhao, T.-L. Teng, and M. Nakamura (2008). A comprehensive relocation of earthquakes in Taiwan from 1991 to 2005, *Bull. Seismol. Soc. Am.* **98,** doi 10.1785/0120070166.

Wu, Y.-H., C.-C. Chen, and J. B. Rundle (2008). Detecting precursory earthquake migration patterns using the pattern informatics method, *Geophys. Res. Lett.* **35,** L19304, doi 10.1029/2008GL035215.

Wyss, M., A. Hasegawa, S. Wiemer, and N. Umino (1999). Quantitative mapping of precursory seismic quiescence before the 1989, *M* 7.1 off-Sanriku earthquake, Japan, *Ann. Di Geofis.* **42,** 851–869.

Zuniga, F. R., and S. Wiemer (1999). Seismicity patterns: Are they always related to natural causes?, *Pure Appl. Geophys.* **155,** 713–726.

Zuniga, F. R., and M. Wyss (1995). Inadvertent changes in magnitude reported in earthquake catalogs: Their evaluation through *b*-value estimates, *Bull. Seismol. Soc. Am.* **85,** 1858–1866.

Appendix

Verification of M_c Uncertainties Obtained from Bootstrapping

Are the estimated uncertainties in the completeness magnitude obtained from bootstrapping reliable? In particular, are small uncertainties realistic if they are based on small sample sizes? In this appendix, we provide evidence that uncertainty estimates based on bootstrapping are indeed reliable, even for small sample sizes, and that the observed large fluctuations of the standard errors for the same small sample size are an accurate reflection of how well a particular sample of magnitudes can constrain the completeness magnitude.

To do this, we perform a synthetic test: We simulate a large data set of magnitudes with known M_c, draw many random samples of equal size from the synthetic catalog, estimate M_c and its standard error using bootstrapping from each sample, and then compare the obtained M_c with the true M_c for each sample. The observed M_c should be close to the true M_c if the estimated uncertainty is small, and vice versa.

The synthetic FMD is based on the model of Ogata and Katsura (1993), according to which, the intensity rate $\lambda(M)$ at magnitude M is given by the product of the intensity rate $\lambda_0(M)$ expected by the Gutenberg–Richter law and a network detection rate $q(M)$:

$$\lambda(M) = \lambda_0(M) \times q(M|\mu,\sigma) = \exp(-\beta M) \times \int_{-\infty}^{M} \frac{1}{\sqrt{2\pi}\sigma} \exp\frac{-(X-\mu)^2}{2\sigma^2} dx, \tag{A1}$$

where β is the b value in the log(10) scale, μ stands for the magnitude at which 50% of earthquakes of magnitude M are detected, and σ characterizes the sharpness of the transition from unlikely to likely detection. Kagan (2002) argued that the Ogata and Katsura model (Ogata and Katsura, 1993) should be used with caution because it assumes statistical stability of the unreliable, only partially detected range of the data set and a particular parametric detection probability rate. But for the purposes of this synthetic test, in which we seek to determine the reliability of uncertainty estimates based on bootstrapping for different sample sizes, these concerns should not matter. Their model is a reasonable approximation to observed FMDs, and that is all we require here.

We set the parameter values of the FMD to $b = 1$, $\mu = 2$, and $\sigma = 0.3$ and simulate a total number of events N_{total} of more than 10,000. We next select $N_r = 1000$ random samples (denoted by i_n) of equal sample size n from the synthetic data set and repeat this random selection of samples for increasing sample size, $n = [4, 5, 6, 7, 8, 9, 10, 20, 50, 100, 500, 1000]$. For each random sample i_n of size n, we estimate the completeness magnitude $M_c^{i,n}$ and its uncertainty $\sigma_0^{i,n}$ by using the MAXC technique: Each sample i_n is bootstrapped (with replacement) $N_s = 200$ times to compute $M_c^{i,n}$ (the mean of the 200 MAXC estimates of M_c) and $\sigma_0^{i,n}$ (the standard error of the 200 MAXC estimates of M_c).

To measure the distance between the estimated and the true M_c, we define the following metric:

$$\varepsilon^{i,n} = \frac{|M_c^{i,n} - M_c|}{\sigma_0^{i,n}}, \tag{A2}$$

where $\varepsilon^{i,n}$ is the absolute error of the M_c estimate based on the ith sample of size n, normalized by the corresponding estimated uncertainty. If the estimated uncertainty $\sigma_0^{i,n}$ is reliable, then the distribution $P_n(\varepsilon)$ of normalized absolute errors should approximate a one-sided Gaussian distribution for each sample size n. In particular, the 0.68, 0.95, and 0.99 percentiles of the distribution $P_n(\varepsilon)$ should be equal to 1, 2, and 3, respectively.

Figure A1 shows the 0.68, 0.95, and 0.99 percentiles of $P_n(\varepsilon)$ versus the sample size n. By assuming a normal

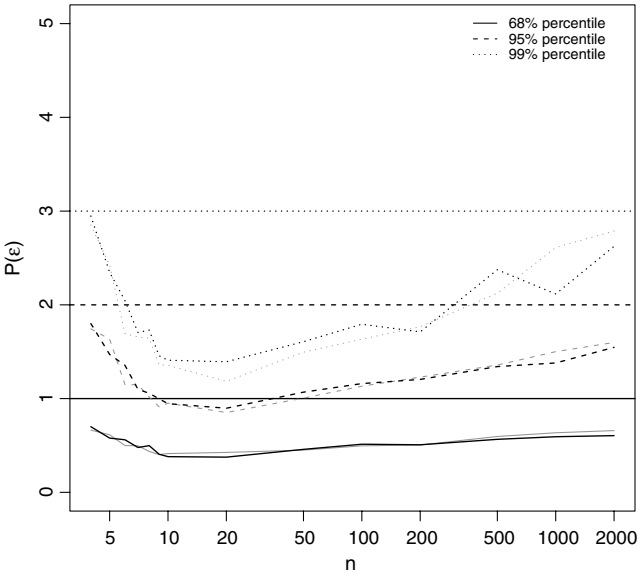

Figure A1. The 0.68, 0.95, and 0.99 percentiles of the normalized absolute error distribution $P_n(\varepsilon)$ versus sample size n. The 0.68, 0.95, and 0.99 percentiles are lower than 1, 2, and 3, respectively, for any sample size n, suggesting that bootstrapping overpredicts M_c uncertainties and provides conservative estimates of σ_0 when assuming Gaussian uncertainties of M_c^{obs}. The parameter ε (equation A2) is computed from $N_s = 200$ bootstrap samples (in black) and from $N_s = 1000$ (in gray).

distribution of the M_c estimates with standard deviation σ_0, bootstrapping overpredicts uncertainties for all sample sizes ranging from $n = 4$ to $n = 1000$ at the 99% or 3σ level when considering a reasonable FMD model (Ogata and Katsura, 1993). We verified that these results, obtained for $N_s = 200$ bootstrap samples, did not vary significantly for larger N_s ($N_s = 1000$, represented in gray in Fig. A1).

The result that bootstrapping gives conservative uncertainty estimates at any sample size n is based on three assumptions, namely, that the FMD model by Ogata and Katsura (1993) and our chosen parameters are a realistic model of the magnitude distribution anywhere (which might not be true in volcanic regions), that self-similarity holds in a volume as small as our chosen cell size (minimum area of $0.05° \times 0.05°$ in Taiwan), and that M_c can be defined as the magnitude bin with the highest frequency of events in the noncumulative FMD (MAXC definition). For other techniques (MBASS, EMR, and GFT), bootstrapping uncertainty appears unreliable for small sample sizes ($n < 100$–200).

Swiss Seismological Service
Institute of Geophysics
ETH-Zürich, Switzerland
(A.M., M.J.W., S.W.)

Department of Earth Sciences
National Central University
Taiwan
(C.-C.C.)

Department of Geosciences
National Taiwan University
Taiwan
(Y.-M.W.)

Manuscript received 15 August 2010